

Nonfactorizable contributions to $B \rightarrow D^{(*)}M$ decays

Yong-Yeon Keum^{a*}, T. Kurimoto^{b†}, Hsiang-nan Li^{c,d‡},
Cai-Dian Lü^{e§}, and A.I. Sanda^{a¶}

^a*Department of Physics, Nagoya University, Nagoya, Japan*

^b*Faculty of Science, Toyama University, Toyama 930-8555, Japan*

^c*Institute of Physics, Academia Sinica, Taipei, Taiwan 115, Republic of China*

^d*Department of Physics, National Cheng-Kung University,
Tainan, Taiwan 701, Republic of China*

^e*CCAST (World Laboratory), P.O. Box 8730, Beijing 100080, China;*

^e*Institute of High Energy Physics, CAS, P.O. Box 918(4), Beijing 100039, China*^{||}

Abstract

While the factorization assumption works well for many two-body nonleptonic B meson decay modes, the recent measurement of $\bar{B} \rightarrow D^{(*)0}M^0$ with $M = \pi, \rho$ and ω shows large deviation from this assumption. We analyze the $B \rightarrow D^{(*)}M$ decays in the perturbative QCD approach based on k_T factorization theorem, in which both factorizable and nonfactorizable contributions can be calculated in the same framework. Our predictions for the Bauer-Stech-Wirbel parameters, $|a_2/a_1| = 0.43 \pm 0.04$ and $Arg(a_2/a_1) \sim -42^\circ$ and $|a_2/a_1| = 0.47 \pm 0.05$ and $Arg(a_2/a_1) \sim -41^\circ$, are consistent with the observed $B \rightarrow D\pi$ and $B \rightarrow D^*\pi$ branching ratios, respectively. It is observed that the large magnitude $|a_2|$ and the large relative phase between a_2 and a_1 come from color-suppressed nonfactorizable amplitudes. Our predictions for the $\bar{B}^0 \rightarrow D^{(*)0}\rho^0, D^{(*)0}\omega$ branching ratios can be confronted with future experimental data.

*yykeum@eken.phys.nagoya-u.ac.jp

†krmt@k2.sci.toyama-u.ac.jp

‡hnli@phys.sinica.edu.tw

§lucd@ihep.ac.cn

¶sanda@eken.phys.nagoya-u.ac.jp

|| Mailing address

1 INTRODUCTION

Understanding nonleptonic B meson decays is crucial for testing the standard model, and also for uncovering the trace of new physics. The simplest case is two-body nonleptonic B meson decays, for which Bauer, Stech and Wirbel (BSW) proposed the factorization assumption (FA) in their pioneering work [1]. Considerable progress, including the generalized FA [2, 3, 4] and QCD-improved FA (QCDF) [5], has been made since this proposal. On the other hand, technique to analyze hard exclusive hadronic scattering was developed by Brodsky and Lepage [6] based on collinear factorization theorem in perturbative QCD (PQCD). A modified framework based on k_T factorization theorem was then given in [7, 8], and extended to exclusive B meson decays in [9, 10, 11, 12]. The infrared finiteness and gauge invariance of k_T factorization theorem was shown explicitly in [13]. Using this so-called PQCD approach, we have investigated dynamics of nonleptonic B meson decays [14, 15, 16]. Our observations are summarized as follows:

1. FA is approximately correct, as our computation shows that nonfactorizable contributions in charmless B meson decays are negligible.
2. Penguin amplitudes are enhanced, as the PQCD formalism includes dynamics from the region, where the energy scale μ runs to $\sqrt{\bar{\Lambda}m_b} < m_b/2$, $\bar{\Lambda} \equiv m_B - m_b$ being the B meson and b quark mass difference.
3. Annihilation diagrams contribute to large short-distance strong phases through the $(S + P)(S - P)$ penguin operators.
4. The sign and magnitude of CP asymmetries in two-body nonleptonic B meson decays can be calculated, and we have predicted relatively large CP asymmetries in the $B \rightarrow K^{(*)}\pi$ [14, 17] and $\pi\pi$ modes [15, 16, 18].

All analyses involving strong dynamics suffer large theoretical uncertainties than we would like. How reliable are these predictions? This can be answered only by comparing more of our predictions with experimental data. For this purpose, we study the $B \rightarrow D^{(*)}M$ decays in PQCD, where M is a pseudoscalar or vector meson. A $D^{(*)}$ meson is massive, and the energy release involved in two-body charmed decays is not so large. If predictions for these decays agree reasonably well with experimental data, PQCD should be more convincing for two-body charmless decays. Since penguin diagrams do not contribute, there are less theoretical ambiguities, such as the argument on chiral enhancement or dynamical enhancement. Checking the validity of PQCD analyses in charmed decays is then more direct.

Note that FA is expected to break down for charmed nonleptonic B meson decays [19]. FA holds for charmless decays because of the color transparency argument: contributions from the dominant soft region cancel between the two nonfactorizable diagrams, where the exchanged gluons attach the quark and the antiquark of the light meson emitted from the weak vertex. For charmed decays with the light meson replaced by a $D^{(*)}$ meson, the two nonfactorizable amplitudes do not cancel due to the mass difference between the two constituent quarks of the $D^{(*)}$ meson. Hence, nonfactorizable contributions ought to be important. This observation further leads to the speculation that strong phases in the $B \rightarrow D^{(*)}M$ decays, if there are any, arise from nonfactorizable amplitudes. In charmless decays, strong phases come from

annihilation amplitudes through the $(S + P)(S - P)$ penguin operators, since nonfactorizable ones are negligible as explained above. The source of strong phases for charmed decays should be different: annihilation amplitudes are small because the $(S + P)(S - P)$ penguin operators are not involved. Nonfactorizable amplitudes could be sizable with a weaker soft cancellation.

In this paper we shall apply the PQCD formalism to the two-body charmed decays $B \rightarrow D^{(*)}M$ with $M = \pi, \rho$ and ω . PQCD has predicted the strong phases from annihilation amplitudes for charmless decays, which are consistent with the recently measured CP asymmetries in the $B_d^0 \rightarrow \pi^+\pi^-$ modes. It is then interesting to examine whether PQCD also gives the correct magnitude and strong phases from nonfactorizable amplitudes implied by the isospin relation of the $B \rightarrow D^{(*)}M$ decays. Compared to the work in [11], the contributions from the twist-3 light meson distribution amplitudes and the threshold resummation effect have been included, and more modes analyzed. The power counting rules for charmed B meson decays, constructed in [20], are employed to obtain the leading factorization formulas. It will be shown that nonfactorizable contributions to charmed decays are calculable in PQCD, and play an important role in explaining the isospin relation indicated by experimental data. The predictions for the $B \rightarrow D^{(*)0}\rho^0, D^{(*)0}\omega$ branching ratios can be confronted with future measurement.

In Sec. II we review the progresses on the study of two-body charmed nonleptonic B meson decays in the literature. The PQCD analysis of the above decays is presented in Sec. III by taking the $B \rightarrow D\pi$ modes as an example. Numerical results for all the $B \rightarrow D^{(*)}M$ branching ratios, and for the extracted BSW parameters a_1 and a_2 are collected in Sec. IV. Sec. V is the conclusion.

2 REVIEW OF PREVIOUS WORKS

2.1 PQCD Approach to $B \rightarrow D^{(*)}$ Form Factors

To develop the PQCD formalism for charmed B meson decays, we have investigated the $B \rightarrow D^{(*)}$ transition form factors in the large recoil region of the $D^{(*)}$ meson [20]. We briefly review this formalism, which serves as the basis of the $B \rightarrow D^{(*)}M$ analyses. The $B \rightarrow D^{(*)}$ transition is more complicated than the $B \rightarrow \pi$ one, because it involves three scales: the B meson mass m_B , the $D^{(*)}$ meson mass $m_{D^{(*)}}$, and the heavy meson and heavy quark mass difference, $\bar{\Lambda} = m_B - m_b \sim m_{D^{(*)}} - m_c$ of order of the QCD scale Λ_{QCD} , $m_{D^{(*)}}$ (m_c) being the $D^{(*)}$ meson (c quark) mass. We have postulated the hierarchy of the three scales,

$$m_B \gg m_{D^{(*)}} \gg \bar{\Lambda}, \quad (1)$$

which allows a consistent power expansion in $m_{D^{(*)}}/m_B$ and in $\bar{\Lambda}/m_{D^{(*)}}$.

Write the B ($D^{(*)}$) meson momentum P_1 (P_2) in the light-cone coordinates as

$$P_1 = \frac{m_B}{\sqrt{2}}(1, 1, \mathbf{0}_T), \quad P_2 = \frac{m_B}{\sqrt{2}}(1, r^2, \mathbf{0}_T), \quad (2)$$

with the mass ratio $r \equiv m_{D^{(*)}}/m_B$. The picture associated with the $B \rightarrow D^{(*)}$ transition is shown in Fig. 1, where the initial state is approximated by the $b\bar{d}$ component. The b quark decays into a c quark and a virtual W boson, which carries the momentum q . Since the constituents are roughly on the mass shell, we have the invariant masses $k_i^2 \sim O(\bar{\Lambda}^2)$, $i = 1$ and

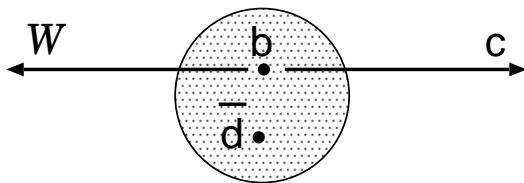


Figure 1: $B \rightarrow D^{(*)}$ transition through the b quark decay into a c quark and a virtual W boson.

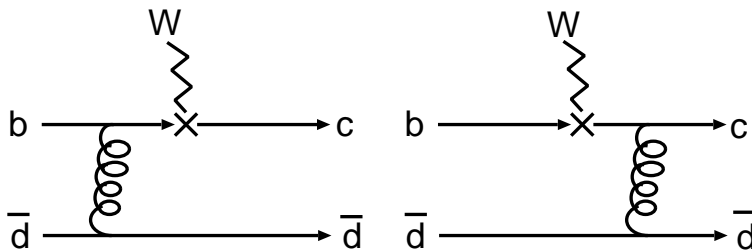


Figure 2: Lowest-order diagrams contributing to the $B \rightarrow D^{(*)}$ form factors. Quite a bit of momentum must be transferred to the spectator \bar{d} quark through the hard gluon exchange.

2, where k_1 (k_2) is the momentum of the spectator \bar{d} quark in the B ($D^{(*)}$) meson. The above kinematic constraints lead to the order of magnitude of k_1 and k_2 [20],

$$\begin{aligned} k_1^\mu &\sim (\bar{\Lambda}, \bar{\Lambda}, \bar{\Lambda}), \\ k_2^\mu &\sim \left(\frac{m_B}{m_{D^{(*)}}} \bar{\Lambda}, \frac{m_{D^{(*)}}}{m_B} \bar{\Lambda}, \bar{\Lambda} \right). \end{aligned} \quad (3)$$

The lowest-order diagrams contributing to the $B \rightarrow D^{(*)}$ form factors contain a hard gluon exchange between the b or c quark and the \bar{d} quark as shown in Fig. 2. The \bar{d} quark undergoes scattering in order to catch up with the c quark, forming a $D^{(*)}$ meson. With the parton momenta in Eq. (3), the exchanged gluon is off-shell by

$$(k_1 - k_2)^2 \sim -\frac{m_B}{m_{D^{(*)}}} \bar{\Lambda}^2, \quad (4)$$

which has been identified as the characteristic scale of the hard kernels. Under Eq. (1), we have $m_B/m_{D^{(*)}} \gg 1$, and the hard kernel is calculable in perturbation theory. It has been found that the applicability of PQCD to the $B \rightarrow D^{(*)}$ transition at large recoil is marginal for the physical masses m_B and $m_{D^{(*)}}$ [20].

Infrared divergences arise from higher-order corrections to Fig. 2. The soft (collinear) type of divergences is absorbed into the B ($D^{(*)}$) meson wave function $\phi_B(x_1, b_1)$ ($\phi_{D^{(*)}}(x_2, b_2)$), which is not calculable but universal. The impact parameter b_1 (b_2) is conjugate to the transverse momentum k_{1T} (k_{2T}) carried by the \bar{d} quark in the B ($D^{(*)}$) meson. It has been shown, from equations of motion for the relevant nonlocal matrix elements, that $\phi_B(x_1, b_1)$ ($\phi_{D^{(*)}}(x_2, b_2)$) has a peak at the momentum fraction $x_1 \equiv k_1^-/P_1^- \sim \bar{\Lambda}/m_B$ ($x_2 \equiv k_2^+/P_2^+ \sim \bar{\Lambda}/m_{D^{(*)}}$) [20].

The form factors are then expressed as the convolution of the hard kernel H with the B and $D^{(*)}$ meson wave functions in k_T factorization theorem,

$$F^{BD^{(*)}}(q^2) = \int dx_1 dx_2 d^2b_1 d^2b_2 \phi_B(x_1, b_1) H(x_1, x_2, b_1, b_2) \phi_{D^{(*)}}(x_2, b_2). \quad (5)$$

The $D^{(*)}$ meson wave function contains a Sudakov factor arising from k_T resummation, which sums the large double logarithms $\alpha_s \ln^2(m_B b_2)$ to all orders. The B meson wave function also contains such a Sudakov factor, whose effect is negligible because a B meson is dominated by soft dynamics. The hard kernel involves a Sudakov factor from threshold resummation, which sums the large double logarithm $\alpha_s \ln^2 x_1$ or $\alpha_s \ln^2 x_2$ to all orders. This factor modifies the end-point behavior of the B and $D^{(*)}$ meson wave functions effectively, rendering them diminish faster in the small $x_{1,2}$ region.

2.2 End-point Singularity and Sudakov Factor

It has been pointed out that if evaluating Fig. 2 in collinear factorization theorem, end-point singularities appear [21]. In this theorem we have the lowest-order hard kernel,

$$H^{(0)}(x_1, x_2) \propto \frac{1}{x_1 x_2}, \quad (6)$$

from the left diagram in Fig. 2, which leads to a logarithmic divergence, as the $D^{(*)}$ meson distribution amplitude behaves like $\phi_{D^{(*)}}(x_2) \propto x_2(1-x_2)$. These singularities imply the breakdown of collinear factorization, and k_T factorization becomes more appropriate. Once the parton transverse momenta k_T are taken into account, Eq. (6) is modified into

$$H^{(0)}(x_1, x_2, \mathbf{k}_{1T}, \mathbf{k}_{2T}) \propto \frac{m_B^4}{[x_1 x_2 m_B^2 + (\mathbf{k}_{1T} - \mathbf{k}_{2T})^2][x_2 m_B^2 + \mathbf{k}_{2T}^2]}. \quad (7)$$

We emphasize that the final state in a $B \rightarrow D^{(*)}$ transition at large recoil does not contain any other hadrons. If it does, it will not manifest itself as the state containing a single $D^{(*)}$ meson. Hence, the transition amplitude must involve a factor, which is related to the probability for the quarks in hard scattering not to emit real gluons. In QED it is a well-known Sudakov suppression factor, an amplitude for an electron not to emit a photon in hard scattering. In the current QCD case, it is the $c\bar{d}$ quark-antiquark color dipole that undergoes hard scattering. At a large separation b between c and \bar{d} , the probability for this large color dipole not to radiate is also suppressed by a Sudakov factor. That is, the configuration with a smaller separation b or with a larger relative transverse momentum k_T is preferred in a $B \rightarrow D^{(*)}$ transition at large recoil. Then the virtual particles involved in the hard kernel remain sufficiently off-shell, and Eq. (5) is free from the end-point singularities.

The corresponding Sudakov factor can be derived in PQCD as a function of the transverse separation b and of the momentum fraction x carried by the spectator quark [9], whose behavior is shown in Fig. 3. The Sudakov factor suppresses the large b region, where the quark and antiquark are separated by a large transverse distance and the color shielding is not so effective. It also suppresses the $x \sim 1$ region, where a quark carries all of the meson momentum, and intends to emit real gluons in hard scattering. The Sudakov factors from k_T resummation [22]

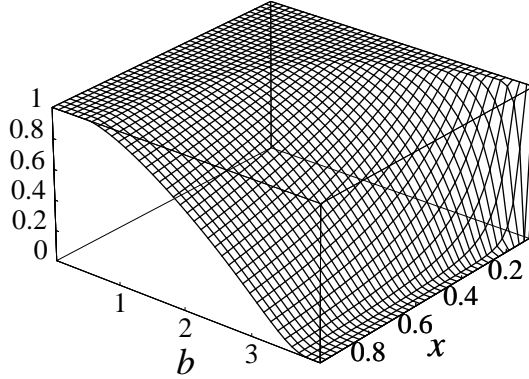


Figure 3: QCD demands the presence of a Sudakov factor. It is an amplitude for a quark-antiquark color dipole not to emit real gluons in the final state. For a large transverse separation b , the quark and antiquark do not shield each other's color charge, and intend to radiate. If it happens, the final state is no longer a single $D^{(*)}$ meson.

for the B and $D^{(*)}$ mesons are only associated with the light spectator quarks, since the double logarithms arise from the overlap of the soft and mass (collinear) divergences. These factors, being universal, are the same as in all our previous analyses.

Similarly, the small x region corresponds to a configuration with a soft spectator, i.e., with a large color dipole in the longitudinal direction. The probability for this large color dipole not to radiate in hard scattering is also described by a Sudakov factor, which comes from threshold resummation for the hard kernels. For the derivation of this Sudakov factor, refer to [23]. For convenience, it has been parametrized as [24],

$$S_t(x) = \frac{2^{1+2e}\Gamma(3/2+c)}{\sqrt{\pi}\Gamma(1+c)}[x(1-x)]^c, \quad (8)$$

with the constant $c = 0.35$. The above parametrization is motivated by the qualitative behavior of S_t : $S_t(x) \rightarrow 0$ as $x \rightarrow 0, 1$ [23]. Since threshold resummation is associated with the hard kernels, the result could be process-dependent. It has been observed that [25] its effect is essential for factorizable decay topologies, and negligible for nonfactorizable decay topologies.

2.3 Factorization Assumption

We review the basics of FA for the $B \rightarrow D^{(*)}M$ decays. The relevant effective weak Hamiltonian is given by

$$\mathcal{H}_{\text{eff}} = \frac{G_F}{\sqrt{2}} V_{cb}V_{ud}^* [C_1(\mu)O_1(\mu) + C_2(\mu)O_2(\mu)], \quad (9)$$

where the four-fermion operators are

$$O_1 = (\bar{d}b)_{V-A}(\bar{c}u)_{V-A}, \quad O_2 = (\bar{c}b)_{V-A}(\bar{d}u)_{V-A}, \quad (10)$$

with the definition $(\bar{q}_1 q_2)_{V-A} \equiv \bar{q}_1 \gamma_\mu (1 - \gamma_5) q_2$, and the Wilson coefficients C_1 and C_2 . The $\bar{B}^0 \rightarrow D^+ \pi^-$ mode is referred to as the class-1 (color-allowed) topology, in which the charged pion is emitted at the weak vertex. The $\bar{B}^0 \rightarrow D^0 \pi^0$ mode is referred to as the class-2 (color-suppressed) topology, in which the D^0 meson is directly produced.

For the $\bar{B}^0 \rightarrow D^+ \pi^-$ mode, O_2 and Fierz transformed O_1 contribute. For the $\bar{B}^0 \rightarrow D^0 \pi^0$ mode, O_1 and Fierz transformed O_2 contribute. Applying FA [1] or generalized FA [2, 3, 4]** to the hadronic matrix elements, we have

$$\begin{aligned} \langle D^+ \pi^- | (\bar{c}b)_{V-A} (\bar{d}u)_{V-A} | \bar{B}^0 \rangle &\approx \langle D^+ | (\bar{c}b)_{V-A} | \bar{B}^0 \rangle \langle \pi^- | (\bar{d}u)_{V-A} | 0 \rangle, \\ \langle D^0 \pi^0 | (\bar{d}b)_{V-A} (\bar{c}u)_{V-A} | \bar{B}^0 \rangle &\approx \langle \pi^0 | (\bar{d}b)_{V-A} | \bar{B}^0 \rangle \langle D^0 | (\bar{c}u)_{V-A} | 0 \rangle. \end{aligned} \quad (11)$$

Substituting the definition of the B meson transition form factors and of the meson decay constants, the $\bar{B}^0 \rightarrow D^+ \pi^-$ (class-1) and $\bar{B}^0 \rightarrow D^0 \pi^0$ (class-2) decay amplitudes are expressed as

$$A(\bar{B}^0 \rightarrow D^+ \pi^-) = i \frac{G_F}{\sqrt{2}} V_{cb} V_{ud}^* (m_B^2 - m_D^2) f_\pi F_0^{BD}(m_\pi^2) a_1(D\pi), \quad (12)$$

$$\sqrt{2} A(\bar{B}^0 \rightarrow D^0 \pi^0) = -i \frac{G_F}{\sqrt{2}} V_{cb} V_{ud}^* (m_B^2 - m_\pi^2) f_D F_0^{B\pi}(m_D^2) a_2(D\pi), \quad (13)$$

where the parameters a_1 and a_2 are defined by

$$a_1 = C_2(\mu) + \frac{C_1(\mu)}{N_c} \quad a_2 = C_1(\mu) + \frac{C_2(\mu)}{N_c}, \quad (14)$$

N_c being the number of colors. The $B^- \rightarrow D^0 \pi^-$ mode, involving both classes of amplitudes, is referred to as class-3. The isospin symmetry implies

$$A(\bar{B}^0 \rightarrow D^+ \pi^-) = A(B^- \rightarrow D^0 \pi^-) + \sqrt{2} A(\bar{B}^0 \rightarrow D^0 \pi^0). \quad (15)$$

It is straightforward to apply FA to other $\bar{B} \rightarrow D^{(*)} M$ modes. a_1 and a_2 depend on the color and Dirac structures of the operators, but otherwise are postulated to be universal [1, 26, 27]. They have the orders of magnitude $a_1(D\pi) \sim O(1)$ and $a_2(D\pi) \sim O(1/N_c)$. The consistency of FA can be tested by comparing a_1 and a_2 extracted from various decays. Within errors, the class-1 decays $\bar{B}^0 \rightarrow D^{(*)+} M^-$ with $M = \pi, \rho, a_1, D_s$, and D_s^* are described using a universal value $|a_1| \approx 1.1 \pm 0.1$, whereas the class-2 decays $\bar{B} \rightarrow \bar{K}^{(*)} M$ with $M = J/\psi$ and $\psi(2S)$ suggest a nearly universal value $|a_2| \approx 0.2-0.3$ [28]. The wide range of $|a_2|$ is due to the uncertainty in the $B \rightarrow K^{(*)}$ form factors. The class-3 decays $B^- \rightarrow D^{(*)0} M^-$ with $M = \pi$ and ρ , which are sensitive to the interference of the two decay topologies, can be explained by a real and positive ratio $a_2/a_1 \approx 0.2-0.3$, which seemed to agree with the determination of $|a_1|$ and $|a_2|$ from other modes. This is the reason FA was claimed to work well in explaining two-body charmed B meson decays, before the class-2 modes $\bar{B}^0 \rightarrow D^0 M^0$ with $M = \pi, \eta$, and ω were measured.

The recently observed $\bar{B}^0 \rightarrow D^0 M^0$ branching ratios listed in Table 1 [29, 30] revealed interesting QCD dynamics. The parameter $|a_2|$ directly extracted from the above modes falls into the range of $|a_2(D\pi)| \sim 0.35 - 0.60$ and $|a_2(D^* \pi)| \sim 0.25 - 0.50$ [31]. To maintain the

**The main difference between FA and generalized FA is that nonfactorizable contributions are included in the latter

predictions for the class-3 decays, there must exist sizeable relative strong phases between class-1 and class-2 amplitudes [19], which are $Arg(a_2/a_1) = 59^\circ$ for the $D\pi$ modes and $Arg(a_2/a_1) = 63^\circ$ for the $D^*\pi$ modes [31]. These results can be regarded as a failure of FA: the parameters a_2 in different types of decays, such as $\bar{B} \rightarrow D^{(*)}\pi$ and $\bar{B} \rightarrow \bar{K}^{(*)}J/\psi$, differ by almost a factor 2 in magnitude, implying strong nonuniversal nonfactorizable effects. It is then crucial to understand this nonuniversality and, especially, the mechanism responsible for the large relative phases in a systematic QCD framework.

3 $B \rightarrow D\pi$ IN PQCD

In this section we take the $B \rightarrow D\pi$ decays as an example of the PQCD analyses. The intensive study of all other modes will be performed in the next section. The $B \rightarrow D\pi$ decay rates have the expressions,

$$\Gamma_i = \frac{1}{128\pi} G_F^2 |V_{cb}|^2 |V_{ud}|^2 \frac{m_B^3}{r} |A_i|^2. \quad (16)$$

The indices for the classes $i = 1, 2$, and 3 , denote the modes $\bar{B}^0 \rightarrow D^+\pi^-$, $\bar{B}^0 \rightarrow D^0\pi^0$, and $B^- \rightarrow D^0\pi^-$, respectively. The amplitudes A_i are written as

$$A_1 = f_\pi \xi_{\text{ext}} + f_B \xi_{\text{exc}} + \mathcal{M}_{\text{ext}} + \mathcal{M}_{\text{exc}}, \quad (17)$$

$$A_2 = -\frac{1}{\sqrt{2}} (f_D \xi_{\text{int}} - f_B \xi_{\text{exc}} + \mathcal{M}_{\text{int}} - \mathcal{M}_{\text{exc}}), \quad (18)$$

$$A_3 = f_\pi \xi_{\text{ext}} + f_D \xi_{\text{int}} + \mathcal{M}_{\text{ext}} + \mathcal{M}_{\text{int}}, \quad (19)$$

where f_B , f_D , and f_π are the B meson, D meson, and pion decay constants, respectively. The functions ξ_{ext} , ξ_{int} , and ξ_{exc} denote the factorizable external W -emission (color-allowed), internal W -emission (color-suppressed), and W -exchange contributions, which come from Figs. 4(a) and 4(b), Figs. 5(a) and 5(b), and Figs. 6(a) and 6(b), respectively. The functions \mathcal{M}_{ext} , \mathcal{M}_{int} , and \mathcal{M}_{exc} represent the nonfactorizable external W -emission, internal W -emission, and W -exchange contributions, which come from Figs. 4(c) and 4(d), Figs. 5(c) and 5(d), and Figs. 6(c) and 6(d), respectively. All the topologies, including factorizable and nonfactorizable ones, have been taken into account. It is easy to find that Eqs. (17)-(19) obey the isospin relation in Eq. (15).

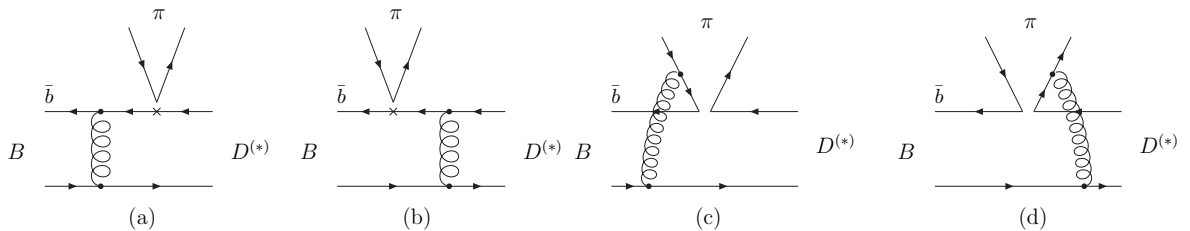


Figure 4: Color-allowed emission diagrams contributing to the $B \rightarrow D^{(*)}\pi$ decays.

In the PQCD framework based on k_T factorization theorem, an amplitude is expressed as the convolution of hard b quark decay kernels with meson wave functions in both the longitudinal momentum fractions and the transverse momenta of partons. Our PQCD formulas are

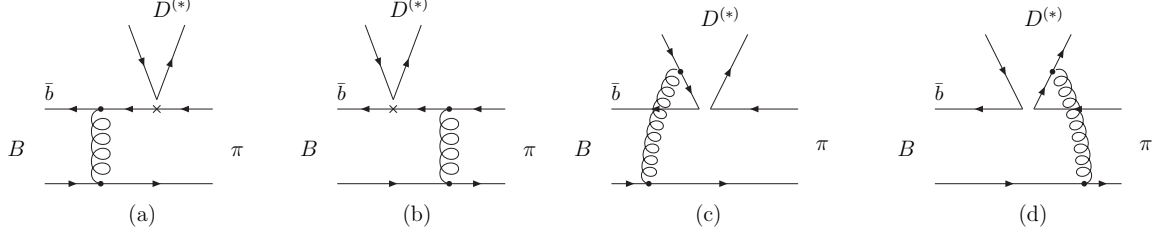


Figure 5: Color-suppressed emission diagrams contributing to the $B \rightarrow D^{(*)}\pi$ decays.

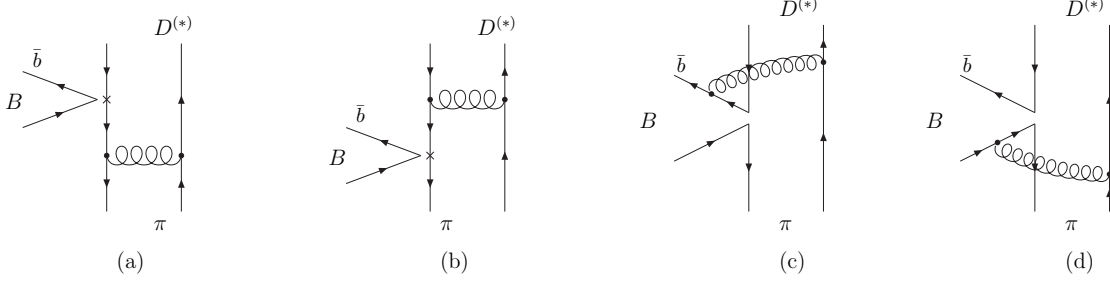


Figure 6: Annihilation Diagrams contributing to the $B \rightarrow D^{(*)}\pi$ decays.

derived up to leading-order in α_s , to leading power in m_D/m_B and in $\bar{\Lambda}/m_D$, and to leading double-logarithm resummations. For the Wilson coefficients, we adopt the leading-order renormalization-group evolution for consistency, although the next-to-leading-order ones are available in the literature [32]. For the similar reason, we employ the one-loop running coupling constant $\alpha_s(\mu) = 2\pi/[\beta_1 \ln(\mu/\Lambda_{\text{QCD}}^{(n_f)})]$ with $\beta_1 = (33 - 2n_f)/3$, n_f being the number of active quarks. The QCD scale is chosen as $\Lambda_{\text{QCD}}^{(5)} = 193$ MeV for the scale $m_b < \mu < m_W$, which is derived from $\Lambda_{\text{QCD}}^{(4)} = 250$ MeV for $\mu < m_b$.

The leading-order and leading-power factorization formulas for the above decay amplitudes are collected in Appendix A. Here we mention only some key ingredients in the calculation. The formulas for the $B \rightarrow D\pi$ decays turn out to be simpler than those for the $B \rightarrow \pi\pi$ ones. The simplicity is attributed to the power counting rules under the hierarchy of the three scales in Eq. (1). The hard kernels are evaluated up to the power corrections of order $\bar{\Lambda}/m_D \sim m_D/m_B$ ($\bar{\Lambda}/m_B$ is regarded as being of even higher power). Following these rules, the terms proportional to $x_1 \sim \bar{\Lambda}/m_B$ and to $x_2 \sim \bar{\Lambda}/m_D$ are higher-power compared to the leading $O(1)$ terms and dropped. We have also dropped the terms of higher powers in $r = m_D/m_B$. Accordingly, the phase space factor $1 - r^2$, appearing in Eq. (16) originally, has been approximated by 1. This approximation is irrelevant for explaining the ratios of the $B \rightarrow D\pi$ branching ratios, and causes an uncertainty in the absolute branching ratios, which is much smaller than those from the CKM matrix element $|V_{cb}|$, and from the meson decay constants f_B and f_D .

Up to the power corrections of order $\bar{\Lambda}/m_B$ and $\bar{\Lambda}/m_D$, we consider only a single B ($D^{(*)}$) meson wave function. The nonperturbative B meson and pion wave functions have been fixed in our previous works [14, 15]. The unknown D meson wave function was determined by fitting the PQCD predictions for the $B \rightarrow D$ transition form factors to the observed $B \rightarrow D l \nu$ decay spectrum [20]. The contributions from the two-parton twist-3 D meson wave functions, being higher-power, are negligible. Note that in the charmless decays the contributions from

the two-parton twist-3 light meson distribution amplitudes are not down by a power of $1/m_B$. These distribution amplitudes, being constant at the momentum fraction $x \rightarrow 0$ as required by equations of motion, lead to linear singularities in the factorization formulas. The linear singularities modify the naive power counting, such that two-parton twist-3 contributions become leading-power [24, 33]. In the charmed decays the above equations of motion are modified [20], and the two-parton twist-3 D meson wave functions vanish at the end point of x . Therefore, their contributions are indeed higher-power.

Retaining the parton transverse momenta k_T , the nonfactorizable topologies generate strong phases from non-pinched singularities of the hard kernels [34]. For example, the virtual quark propagator in Fig. 5(d) is written, in the principle-value prescription, as

$$\frac{1}{x_3(x_2 - x_1)m_B^2 - (\mathbf{k}_{2T} - \mathbf{k}_{1T} + \mathbf{k}_{3T})^2 + i\epsilon} = P \left[\frac{1}{x_3(x_2 - x_1)m_B^2 - (\mathbf{k}_{2T} - \mathbf{k}_{1T} + \mathbf{k}_{3T})^2} \right] - i\pi\delta(x_3(x_2 - x_1)m_B^2 - (\mathbf{k}_{2T} - \mathbf{k}_{1T} + \mathbf{k}_{3T})^2), \quad (20)$$

with x_3 being the momentum fraction associated with the pion. The second term contributes to the strong phase, which is thus of short-distance origin and calculable. The first term in the above expression does not lead to an end-point singularity. Note that the strong phase from Eq. (20) is obtained by keeping all terms in the denominator of a propagator, without neglecting x_1 and x_2 .

4 NUMERICAL RESULTS

The computation of the hard kernels in k_T factorization theorem for other charmed decay modes is similar and straightforward. The $B \rightarrow D^*\pi$ decay amplitudes are the same as the $B \rightarrow D\pi$ ones but with the substitution of the mass, the decay constant, and the distribution amplitude,

$$m_D \rightarrow m_{D^*}, \quad f_D \rightarrow f_{D^*}, \quad \phi_D(x_2) \rightarrow \phi_{D^*}(x_2). \quad (21)$$

This simple substitution is expected at leading power under the hierarchy in Eq. (1): the difference between the two channels should occur only at $O(\bar{\Lambda}/m_D)$. An explicit derivation shows that the difference occurs at the twist-3 level for the nonfactorizable emission diagrams in Fig. 4 and for the annihilation diagrams in Fig. 6. It implies that the universality (channel-independence) of a_1 and a_2 assumed in FA [44] breaks down at subleading power even for the $B \rightarrow D^{(*)}M$ decays.

Replacing the pion in Figs. 4-6 by $\rho(\omega)$ meson, we obtain the diagrams for the $B \rightarrow D^{(*)}\rho(\omega)$ decays. The factorization formulas for the $B \rightarrow D\rho(\omega)$ decay amplitudes are also the same as those for the $B \rightarrow D\pi$ ones but with the substitution,

$$\phi_\pi \rightarrow \phi_{\rho,\omega}, \quad \phi_\pi^p \rightarrow \phi_{\rho,\omega}^s, \quad \phi_\pi^t \rightarrow \phi_{\rho,\omega}^t, \quad m_0 \rightarrow m_{\rho(\omega)}, \quad (22)$$

where ϕ_π ($\phi_\pi^{p,t}$) is the two-parton twist-2 (twist-3) pion distribution amplitudes, $\phi_{\rho,\omega}$ ($\phi_{\rho,\omega}^{s,t}$) the two-parton twist-2 (twist-3) $\rho(\omega)$ meson distribution amplitudes, m_0 the chiral enhancement scale, and $m_{\rho(\omega)}$ the $\rho(\omega)$ meson mass. Hence, the similar isospin relation holds:

$$\mathcal{M}(B^0 \rightarrow D^- \rho^+) = \mathcal{M}(B^+ \rightarrow \bar{D}^0 \rho^+) + \sqrt{2}\mathcal{M}(B^0 \rightarrow \bar{D}^0 \rho^0). \quad (23)$$

The $B \rightarrow D^* \rho(\omega)$ decays contain more amplitudes associated with the different polarizations, whose explicit expressions are referred to Appendix B.

In the numerical analysis we adopt the model for the B meson wave function,

$$\phi_B(x, b) = N_B x^2 (1-x)^2 \exp \left[-\frac{1}{2} \left(\frac{x m_B}{\omega_B} \right)^2 - \frac{\omega_B^2 b^2}{2} \right], \quad (24)$$

with the shape parameter ω_B and the normalization constant N_B being related to the decay constant f_B through

$$\int dx \phi_B(x, 0) = \frac{f_B}{2\sqrt{2N_c}}. \quad (25)$$

The $D^{(*)}$ meson distribution amplitude is given by

$$\phi_{D^{(*)}}(x) = \frac{3}{\sqrt{2N_c}} f_{D^{(*)}} x(1-x) [1 + C_{D^{(*)}}(1-2x)], \quad (26)$$

with the shape parameter $C_{D^{(*)}}$ and the decay constant $f_{D^{(*)}}$. The pion and $\rho(\omega)$ meson distribution amplitudes have been derived in [35, 36], whose explicit expressions are given in Appendix A. The B meson wave function was then extracted from the light-cone sum rule results of the $B \rightarrow \pi$ transition form factor [24]. The range of $C_{D^{(*)}}$ was determined from the measured $B \rightarrow D^{(*)} l \nu$ decay spectrum at large recoil employing the B meson wave function extracted above. We do not consider the variation of $\phi_{D^{(*)}}$ with the impact parameter b , since the available data are not yet sufficiently precise to control this dependence.

The input parameters are listed below:

$$\begin{aligned} f_B &= 190 \text{ MeV}, \quad \omega_B = 0.4 \text{ GeV}, \\ f_D &= 240 \text{ MeV}, \quad C_D = 0.8 \pm 0.2, \\ f_{D^*} &= 230 \text{ MeV}, \quad C_{D^*} = 0.7 \pm 0.2, \\ f_\pi &= 132 \text{ MeV}, \quad f_\rho = f_\omega = 200 \text{ MeV}, \quad f_\rho^T = f_\omega^T = 160 \text{ MeV}, \\ m_B &= 5.28 \text{ GeV}, \quad m_b = 4.8 \text{ GeV}, \\ m_D &= 1.87 \text{ GeV}, \quad m_{D^*} = 2.01 \text{ GeV}, \quad m_c = 1.3 \text{ GeV}, \\ m_\rho &= 0.77 \text{ GeV}, \quad m_\omega = 0.78 \text{ GeV}, \\ m_t &= 170 \text{ GeV}, \quad m_W = 80.41 \text{ GeV}, \quad m_0 = 1.4 \text{ GeV}, \\ \tau_{B^\pm} &= 1.674 \times 10^{-12} \text{ s}, \quad \tau_{B^0} = 1.542 \times 10^{-12} \text{ s}, \\ G_F &= 1.16639 \times 10^{-5} \text{ GeV}^{-2}, \quad |V_{cb}| = 0.043, \quad |V_{ud}| = 0.974, \end{aligned} \quad (27)$$

where m_t , m_W , τ_{B^\pm} and τ_{B^0} denote the top quark mass, the W boson mass, the B^\pm meson lifetime, and the B^0 meson lifetime, respectively. The above meson wave functions and parameters correspond to the form factors at maximal recoil,

$$F_0^{B\pi} \sim 0.3, \quad \xi_+^{BD} \sim 0.57, \quad \xi_{A_1}^{BD^*} \sim 0.52, \quad (28)$$

which are close to the results from the light-cone QCD sum rules [37]. We stress that there is no arbitrary parameter in our calculation, though the value of each parameter is only known up to a range.

The PQCD predictions for each term of the $B \rightarrow D\pi$ decay amplitudes is exhibited in Table 2. The theoretical uncertainty comes only from the variation of the shape parameter for the D meson distribution amplitude, $0.6 < C_D < 1.0$. It is expected that the color-allowed factorizable amplitude $f_\pi \xi_{\text{ext}}$ dominates, and that the color-suppressed factorizable contribution $f_D \xi_{\text{int}}$ is smaller due to the Wilson coefficient $C_1 + C_2/N_c \sim 0$. The color-allowed nonfactorizable amplitude \mathcal{M}_{ext} is negligible: since the pion distribution amplitude is symmetric under the exchange of x_3 and $1 - x_3$, the contributions from the two diagrams Figs. 4(c) and 4(d) cancel each other in the dominant region with small x_2 . It is also down by the small Wilson coefficient C_1/N_c . For the color-suppressed nonfactorizable contribution \mathcal{M}_{int} , the above cancellation does not exist in the dominant region with small x_3 , because the D meson distribution amplitude $\phi_D(x_2)$ is not symmetric under the exchange of x_2 and $1 - x_2$. Furthermore, \mathcal{M}_{int} , proportional to $C_2/N_c \sim 0.3$, is not down by the Wilson coefficient. It is indeed comparable to the color-allowed factorizable amplitude $f_\pi \xi_{\text{ext}}$, and produces a large strong phase as explained in Eq. (20). Both the factorizable and nonfactorizable annihilation contributions are vanishingly small, consistent with our argument in Sec. II.

The predicted branching ratios in Table 3 are in agreement with the averaged experimental data [29, 30, 38]. We extract the parameters a_1 and a_2 by equating Eqs. (12) and (13) to Eqs. (17) and (18), respectively. That is, our a_1 and a_2 do not only contain the nonfactorizable amplitudes as in generalized FA, but the small annihilation amplitudes, which was first discussed in [39]. We obtain the ratio $|a_2/a_1| \sim 0.43$ with 10% uncertainty and the phase of a_2 relative to a_1 about $\text{Arg}(a_2/a_1) \sim -42^\circ$. If excluding the annihilation amplitudes $f_B \xi_{\text{exc}}$ and \mathcal{M}_{exc} , we have $|a_2/a_1| \sim 0.46$ and $\text{Arg}(a_2/a_1) \sim -64^\circ$. Note that the experimental data do not fix the sign of the relative phases. The PQCD calculation indicates that $\text{Arg}(a_2/a_1)$ should be located in the fourth quadrant. It is evident that the short-distance strong phase from the color-suppressed nonfactorizable amplitude is already sufficient to account for the isospin triangle formed by the $B \rightarrow D\pi$ modes. The conclusion that the data hint large final-state interaction was drawn from the analyses based on FA [19, 31, 40, 41]. Hence, it is more reasonable to claim that the data just imply a large strong phase, but do not tell what mechanism generates this phase [42]. From the viewpoint of PQCD, this strong phase is of short distance, and produced from the non-pinched singularity of the hard kernel. Certainly, under the current experimental and theoretical uncertainties, there is still room for long-distance phases from final-state interaction.

At this point it is useful to compare our formalism with the QCDF approach [5] based on collinear factorization theorem. In QCDF a $B \rightarrow D^{(*)}$ transition form factor is not calculable because of the end-point singularity, and has to be parametrized as a soft object, like a non-perturbative meson distribution amplitude. Similarly, the neglect of k_T in Eq. (20) results in an end-point singularity for the amplitude associated with Fig. 5(d). If the c quark is massless, the D meson distribution amplitude $\phi_D(x_2)$ will be symmetric under the exchange of x_2 and $1 - x_2$. The end-point singularities in the pair of color-suppressed nonfactorizable diagrams, Figs. 5(c) and 5(d), cancel each other. This can be understood by checking the behavior of the integrand of \mathcal{M}_{int} in Eq. (40) in the dominant region with small x_3 . However, the nonfactorizable contribution becomes negligible as in the $B \rightarrow \pi\pi$ case [33, 43]. In this limit of $m_c \rightarrow 0$, the amplitude \mathcal{M}_{int} , though calculable in QCDF, is not large enough to explain the $B \rightarrow D\pi$ data. If the c quark is treated as being massive, ϕ_D will not be symmetric, and the end-point singularities do not cancel. \mathcal{M}_{int} , i.e., the magnitude and phase of a_2 , are then not calculable.

The PQCD predictions for the $B \rightarrow D^*\pi$ decay amplitudes and branching ratios in Table 4 are also consistent with the data [45]. Since m_{D^*} and ϕ_{D^*} are slightly different from m_D and ϕ_D , respectively, the results are close to those in Table 3. The $B \rightarrow D^*\pi$ branching ratios are smaller than the $B \rightarrow D\pi$ ones because of the form factors $\xi_{A_1}^{BD^*} < \xi_+^{BD}$ as shown in Eq. (28). Similarly, the ratio $|a_2/a_1|$ and the relative phase $Arg(a_2/a_1)$ are also close to those associated with the $B \rightarrow D\pi$ decays. We obtain the ratio $|a_2/a_1| \sim 0.47$ with 10% uncertainty and the relative phase about $Arg(a_2/a_1) \sim -41^\circ$. If excluding the annihilation amplitudes, we have $|a_2/a_1| \sim 0.51$ and $Arg(a_2/a_1) \sim -63^\circ$. The PQCD predictions for the $B \rightarrow D^{(*)}\rho(\omega)$ branching ratios are listed in Table 5, which well match the data [45]. The predictions for the $B \rightarrow D^{(*)0}\rho^0(\omega)$ decays can be compared with the future measurement.

5 CONCLUSION

In this paper we have analyzed the two-body nonleptonic charmed decays $B \rightarrow D^{(*)}M$ with $M = \pi, \rho,$ and ω in the PQCD approach. This framework is based on k_T factorization theorem, which is free of end-point singularities and gauge-invariant. k_T factorization theorem is more appropriate, when the end-point region of a momentum fraction is important, and collinear factorization theorem breaks down. By keeping the transverse degrees of freedom of partons in the evaluation of a hard kernel, and including the Sudakov factors from k_T and threshold resummations, the virtual particles remain sufficiently off-shell, and the end-point singularities do not exist. When applying this approach to two-body charmless decays, we have predicted large CP asymmetries and dynamical penguin enhancement, which are in agreement with the $B \rightarrow PP$ ($\pi\pi, K\pi$) data and with $B \rightarrow VP$ ($\phi K, K^*\pi$) data, respectively.

The derivation of the factorization formulas for the $B \rightarrow D^{(*)}M$ decay amplitudes follow the power counting rules constructed in our previous work on the $B \rightarrow D^{(*)}$ transition form factors. Under the hierarchy $m_B \gg m_{D^{(*)}} \gg \bar{\Lambda}$, the B and $D^{(*)}$ meson wave functions exhibit a peak at the momentum fractions around $\bar{\Lambda}/m_B$ and $\bar{\Lambda}/m_{D^{(*)}}$, respectively. Up to leading power in $m_{D^{(*)}}/m_B$ and in $\bar{\Lambda}/m_{D^{(*)}}$, only a single B meson wave function and a single $D^{(*)}$ meson wave function are involved. The factorization formulas then become very simple compared to those for the charmless decays. Moreover, the factorization formulas for all the $B \rightarrow D^{(*)}M$ modes are identical, except the appropriate substitution of the masses, the decay constants, and the meson distribution amplitudes.

Being free from the end-point singularities, all topologies of decay amplitudes are calculable in PQCD, including the color-suppressed nonfactorizable one. This amplitude can not be computed in QCDF based on collinear factorization theorem because of the existence of the end-point singularities for a massive c quark. We observed in PQCD that this amplitude, not suppressed by the Wilson coefficient (proportional to C_2/N_c), is comparable to the dominant color-allowed factorizable amplitude. It generates a large strong phase from the non-pinched singularity of the hard kernel, which is crucial for explaining the observed $B \rightarrow D^{(*)}M$ branching ratios. The color-allowed nonfactorizable contribution is negligible because of the pair cancellation and the small Wilson coefficient C_1/N_c . The color-suppressed factorizable amplitude is negligible due to the small Wilson coefficient $a_2 = C_1 + C_2/N_c$. The annihilation amplitudes are not important, since they occur through the tree operators.

As stated before, we have predicted the large strong phases from the scalar-penguin annihilation amplitudes, which are required by the large CP asymmetries in two-body charmless

decays. The success in predicting the strong phases from the color-suppressed nonfactorizable amplitudes for the two-body charmed decays further supports k_T factorization theorem. The conclusion drawn in this work is that the short-distance strong phase is already sufficient to account for the $B \rightarrow D^{(*)}M$ data. Certainly, there is still room for long-distance strong phases from final-state interaction. We emphasize that there is no arbitrary parameter in our analysis (there are in QCDF), though all universal inputs are not yet known precisely. The meson wave functions have been determined either from the semileptonic data or from light-cone QCD sum rules. All our predictions are consistent with the existing measurements. For those without data, such as the $B \rightarrow D^{*0}\rho^0(\omega)$ modes, our predictions can be confronted with the future measurement. For the application of the PQCD approach to other charmed decays, such as $B \rightarrow D_s^{(*)}K$ and $B \rightarrow D^{(*)}f_0$, refer to [46] and [47], respectively.

Acknowledgments

The authors are grateful to the organizers of Summer Institute 2002 at Fuji-Yoshida, Japan, where part of this work was done, for warm hospitality. This work was supported by the Japan Society for the Promotion of Science (Y.Y.K.), by Grant-in Aid for Scientific Research from the Japan Society for the Promotion of Science under the Grant No. 11640265 (T.K.), by the National Science Council of R.O.C. under the Grant No. NSC-91-2112-M-001-053 (H-n.L.), by the National Science Foundation of China under Grants No. 90103013 and 10135060 (C.D.L.), and by Ministry of Education, Science and Culture, Japan (A.I.S.).

A FACTORIZATION FORMULAS FOR $B \rightarrow D\pi$

In this Appendix we present the factorization formulas for the $B \rightarrow D\pi$ decay amplitudes. We choose the B meson, D meson, and pion momenta in the light-cone coordinate as,

$$P_1 = \frac{m_B}{\sqrt{2}}(1, 1, \mathbf{0}_T), \quad P_2 = \frac{m_B}{\sqrt{2}}(1, r^2, \mathbf{0}_T), \quad P_3 = \frac{m_B}{\sqrt{2}}(0, 1 - r^2, \mathbf{0}_T), \quad (29)$$

respectively, with $r = m_D/m_B$ being defined before. The fractional momenta of the light valence quarks in the B meson, D meson and the pion are

$$\begin{aligned} k_1 &= x_1 \frac{m_B}{\sqrt{2}}(1, 0, \mathbf{0}_T) + \mathbf{k}_{1T} \quad \text{for } \xi_{\text{int}}, M_{\text{int}}, \\ k_1 &= x_1 \frac{m_B}{\sqrt{2}}(0, 1, \mathbf{0}_T) + \mathbf{k}_{1T} \quad \text{for others,} \\ k_2 &= x_2 \frac{m_B}{\sqrt{2}}(1, 0, \mathbf{0}_T) + \mathbf{k}_{2T}, \\ k_3 &= x_3 \frac{m_B}{\sqrt{2}}(0, 1 - r^2, \mathbf{0}_T) + \mathbf{k}_{3T}, \end{aligned} \quad (30)$$

respectively. Which longitudinal component of k_1 , k_1^+ or k_1^- , is relevant depends on the final-state meson the hard gluon attaches. That is, it is selected by the inner product $k_1 \cdot k_3$ or $k_1 \cdot k_2$.

The factorizable amplitudes ξ_{ext} , ξ_{int} and ξ_{exc} are written as

$$\begin{aligned} \xi_{\text{ext}} &= 16\pi C_F \sqrt{r} m_B^2 \int_0^1 dx_1 dx_2 \int_0^{1/\Lambda} b_1 db_1 b_2 db_2 \phi_B(x_1, b_1) \phi_D(x_2) \\ &\quad \times \{E_e(t_e^{(1)})h(x_1, x_2, b_1, b_2)S_t(x_2) + r E_e(t_e^{(2)})h(x_2, x_1, b_2, b_1)S_t(x_1)\}, \end{aligned} \quad (31)$$

$$\begin{aligned} \xi_{\text{int}} &= 16\pi C_F \sqrt{r} m_B^2 \int_0^1 dx_1 dx_3 \int_0^{1/\Lambda} b_1 db_1 b_3 db_3 \phi_B(x_1, b_1) \\ &\quad \times \{[(1+x_3)\phi_\pi(x_3) + r_0(1-2x_3)(\phi_\pi^p(x_3) + \phi_\pi^t(x_3))] \\ &\quad \times E_i(t_i^{(1)})h(x_1, x_3(1-r^2), b_1, b_3)S_t(x_3) \\ &\quad + 2r_0\phi_\pi^p(x_3)E_i(t_i^{(2)})h(x_3, x_1(1-r^2), b_3, b_1)S_t(x_1)\}, \end{aligned} \quad (32)$$

$$\begin{aligned} \xi_{\text{exc}} &= 16\pi C_F \sqrt{r} m_B^2 \int_0^1 dx_2 dx_3 \int_0^{1/\Lambda} b_2 db_2 b_3 db_3 \phi_D(x_2) \\ &\quad \times \{-x_3\phi_\pi(x_3)E_a(t_a^{(1)})h_a(x_2, x_3(1-r^2), b_2, b_3)S_t(x_3) \\ &\quad + x_2\phi_\pi(x_3)E_a(t_a^{(1)})h_a(x_3, x_2(1-r^2), b_3, b_2)S_t(x_2)\}, \end{aligned} \quad (33)$$

with the mass ratio $r_0 \equiv m_0/m_B$ and the evolution factors,

$$\begin{aligned} E_e(t) &= \alpha_s(t)a_1(t) \exp[-S_B(t) - S_D(t)], \\ E_i(t) &= \alpha_s(t)a_2(t) \exp[-S_B(t) - S_\pi(t)], \\ E_a(t) &= \alpha_s(t)a_2(t) \exp[-S_D(t) - S_\pi(t)], \end{aligned} \quad (34)$$

and the Wilson coefficients,

$$a_1 = C_2 + \frac{C_1}{N_c}, \quad a_2 = C_1 + \frac{C_2}{N_c}. \quad (35)$$

Note that $C_1 = 0$ and $C_2 = 1$ at tree level in our convention. The explicit expressions of the Sudakov factors $\exp[-S_B(t)]$, $\exp[-S_D(t)]$ and $\exp[-S_\pi(t)]$ from k_T resummation are referred to [24, 20].

The functions h 's, obtained from Figs. 4(a) and 4(b), Figs. 5(a) and 5(b), and Figs. 6(a) and 6(b), are given by

$$\begin{aligned} h(x_1, x_2, b_1, b_2) &= K_0(\sqrt{x_1 x_2} m_B b_1) \\ &\quad \times [\theta(b_1 - b_2)K_0(\sqrt{x_2} m_B b_1) I_0(\sqrt{x_2} m_B b_2) \\ &\quad + \theta(b_2 - b_1)K_0(\sqrt{x_2} m_B b_2) I_0(\sqrt{x_2} m_B b_1)], \end{aligned} \quad (36)$$

$$\begin{aligned} h_a(x_2, x_3, b_2, b_3) &= \left(i\frac{\pi}{2}\right)^2 H_0^{(1)}(\sqrt{x_2 x_3} m_B b_2) \\ &\quad \times [\theta(b_2 - b_3)H_0^{(1)}(\sqrt{x_3} m_B b_2) J_0(\sqrt{x_3} m_B b_3) \\ &\quad + \theta(b_3 - b_2)H_0^{(1)}(\sqrt{x_3} m_B b_3) J_0(\sqrt{x_3} m_B b_2)]. \end{aligned} \quad (37)$$

The hard scales t are chosen as

$$\begin{aligned} t_e^{(1)} &= \max(\sqrt{x_2} m_B, 1/b_1, 1/b_2), \quad t_e^{(2)} = \max(\sqrt{x_1} m_B, 1/b_1, 1/b_2), \\ t_i^{(1)} &= \max(\sqrt{x_3(1-r^2)} m_B, 1/b_1, 1/b_3), \quad t_i^{(2)} = \max(\sqrt{x_1(1-r^2)} m_B, 1/b_1, 1/b_3), \\ t_a^{(1)} &= \max(\sqrt{x_3(1-r^2)} m_B, 1/b_2, 1/b_3), \quad t_a^{(2)} = \max(\sqrt{x_2(1-r^2)} m_B, 1/b_2, 1/b_3). \end{aligned} \quad (38)$$

For the nonfactorizable amplitudes, the factorization formulas involve the kinematic variables of all the three mesons. Their expressions are

$$\begin{aligned} \mathcal{M}_{\text{ext}} &= 32\pi\sqrt{2N}C_F\sqrt{r}m_B^2 \int_0^1 [dx] \int_0^{1/\Lambda} b_1 db_1 b_3 db_3 \phi_B(x_1, b_1) \phi_D(x_2) \phi_\pi(x_3) \\ &\quad \times \left[x_3 E_b(t_b^{(1)}) h_b^{(1)}(x_i, b_i) - (1 - x_3 + x_2) E_b(t_b^{(1)}) h_b^{(2)}(x_i, b_i) \right], \end{aligned} \quad (39)$$

$$\begin{aligned} \mathcal{M}_{\text{int}} &= 32\pi\sqrt{2N}C_F\sqrt{r}m_B^2 \int_0^1 [dx] \int_0^{1/\Lambda} b_1 db_1 b_2 db_2 \phi_B(x_1, b_1) \phi_D(x_2) \\ &\quad \times \left[(-x_2 - x_3) \phi_\pi(x_3) E_d(t_d^{(1)}) h_d^{(1)}(x_i, b_i) + (1 - x_2) \phi_\pi(x_3) E_d(t_d^{(2)}) h_d^{(2)}(x_i, b_i) \right], \end{aligned} \quad (40)$$

$$\begin{aligned} \mathcal{M}_{\text{exc}} &= 32\pi\sqrt{2N}C_F\sqrt{r}m_B^2 \int_0^1 [dx] \int_0^{1/\Lambda} b_1 db_1 b_2 db_2 \phi_B(x_1, b_1) \phi_D(x_2) \\ &\quad \times \left[x_3 \phi_\pi(x_3) E_f(t_f^{(1)}) h_f^{(1)}(x_i, b_i) - x_2 \phi_\pi(x_3) E_f(t_f^{(2)}) h_f^{(2)}(x_i, b_i) \right], \end{aligned} \quad (41)$$

from Figs. 4(c) and 4(d), Figs. 5(c) and 5(d), and Figs. 6(c) and 6(d), respectively, with the definition $[dx] \equiv dx_1 dx_2 dx_3$. The evolution factors are given by

$$\begin{aligned} E_b(t) &= \alpha_s(t) \frac{C_1(t)}{N} \exp[-S(t)|_{b_2=b_1}], \\ E_d(t) &= \alpha_s(t) \frac{C_2(t)}{N} \exp[-S(t)|_{b_3=b_1}], \\ E_f(t) &= \alpha_s(t) \frac{C_2(t)}{N} \exp[-S(t)|_{b_3=b_2}]. \end{aligned} \quad (42)$$

with the Sudakov exponent $S = S_B + S_D + S_\pi$.

The functions $h^{(j)}$, $j = 1$ and 2 , appearing in Eqs. (39)-(41), are written as

$$\begin{aligned} h_b^{(j)} &= [\theta(b_1 - b_3) K_0(Bm_B b_1) I_0(Bm_B b_3) \\ &\quad + \theta(b_3 - b_1) K_0(Bm_B b_3) I_0(Bm_B b_1)] \\ &\quad \times \left(\begin{array}{l} K_0(B_j m_B b_3) \quad \text{for } B_j^2 \geq 0 \\ \frac{i\pi}{2} H_0^{(1)}(\sqrt{|B_j^2|} m_B b_3) \quad \text{for } B_j^2 \leq 0 \end{array} \right), \end{aligned} \quad (43)$$

$$\begin{aligned} h_d^{(j)} &= [\theta(b_1 - b_2) K_0(Dm_B b_1) I_0(Dm_B b_2) \\ &\quad + \theta(b_2 - b_1) K_0(Dm_B b_2) I_0(Dm_B b_1)] \\ &\quad \times \left(\begin{array}{l} K_0(D_j m_B b_2) \quad \text{for } D_j^2 \geq 0 \\ \frac{i\pi}{2} H_0^{(1)}(\sqrt{|D_j^2|} m_B b_2) \quad \text{for } D_j^2 \leq 0 \end{array} \right), \end{aligned} \quad (44)$$

$$\begin{aligned} h_f^{(j)} &= i\frac{\pi}{2} [\theta(b_1 - b_2) H_0^{(1)}(Fm_B b_1) J_0(Fm_B b_2) \\ &\quad + \theta(b_2 - b_1) H_0^{(1)}(Fm_B b_2) J_0(Fm_B b_1)] \\ &\quad \times \left(\begin{array}{l} K_0(F_j m_B b_1) \quad \text{for } F_j^2 \geq 0 \\ \frac{i\pi}{2} H_0^{(1)}(\sqrt{|F_j^2|} m_B b_1) \quad \text{for } F_j^2 \leq 0 \end{array} \right), \end{aligned} \quad (45)$$

with the variables

$$B^2 = x_1 x_2,$$

$$\begin{aligned}
B_1^2 &= x_1 x_2 - x_2 x_3 (1 - r^2) , \\
B_2^2 &= x_1 x_2 - x_2 (1 - x_3) (1 - r^2) , \\
D^2 &= x_1 x_3 (1 - r^2) , \\
D_1^2 &= F_1^2 = (x_1 - x_2) x_3 (1 - r^2) , \\
D_2^2 &= (x_1 + x_2) r^2 - (1 - x_1 - x_2) x_3 (1 - r^2) , \\
F^2 &= x_2 x_3 (1 - r^2) , \\
F_2^2 &= x_1 + x_2 + (1 - x_1 - x_2) x_3 (1 - r^2) .
\end{aligned} \tag{46}$$

There is an ambiguity in defining a light-cone B meson wave function for the nonfactorizable amplitude \mathcal{M}_{exc} , since both the components k_1^+ and k_1^- contribute through the inner products $k_1 \cdot k_2$ and $k_1 \cdot k_3$ in the denominators of the virtual particle propagators. However, a careful examination of the factorization formula shows that the dominant region is the one with $k_2 \sim O(\bar{\Lambda})$ and $k_3 \sim O(m_B)$ at leading twist. Hence, we drop the term $k_1 \cdot k_2$. The scales $t^{(j)}$ are chosen as

$$\begin{aligned}
t_b^{(j)} &= \max(Bm_B, \sqrt{|B_j^2|}m_B, 1/b_1, 1/b_3) , \\
t_d^{(j)} &= \max(Dm_B, \sqrt{|D_j^2|}m_B, 1/b_1, 1/b_2) , \\
t_f^{(j)} &= \max(Fm_B, \sqrt{|F_j^2|}m_B, 1/b_1, 1/b_2) .
\end{aligned} \tag{47}$$

We explain that the factorization formulas presented above are indeed of leading power under the power counting rules in [20]. The factorizable amplitudes are as shown in [20, 33]. For the nonfactorizable amplitudes, the terms proportional to x_3 and to $1 - x_3$ in \mathcal{M}_{ext} cancel each other roughly. This cancellation can be understood by means of the corresponding expression in collinear factorization theorem: the first and second terms in \mathcal{M}_{ext} are proportional to

$$-\frac{x_3}{x_1 x_2^2 x_3} , \quad \frac{1 - x_3 + x_2}{x_1 x_2^2 (1 - x_3)} . \tag{48}$$

For simplicity, x_1 has been suppressed, when it appears in the sum together with x_2 or x_3 . It is found that the first ratio cancels the $1 - x_3$ term in the second ratio. That is, the x_2 term is in fact leading and not negligible. For a similar reason, the $-x_2$ term in \mathcal{M}_{int} cancels the $1 - x_2$ term. Hence, the $-x_3$ term is leading. If one drops $-x_2$ in \mathcal{M}_{int} , the above cancellation disappears, and a fake leading term will be introduced.

The pion and ρ meson distribution amplitudes have been derived in [35, 36]:

$$\phi_\pi(x) = \frac{3f_\pi}{\sqrt{2N_c}} x(1-x) \left[1 + 0.44C_2^{3/2}(2x-1) + 0.25C_4^{3/2}(2x-1) \right] , \tag{49}$$

$$\phi_\pi^p(x) = \frac{f_\pi}{2\sqrt{2N_c}} \left[1 + 0.43C_2^{1/2}(2x-1) + 0.09C_4^{1/2}(2x-1) \right] , \tag{50}$$

$$\phi_\pi^t(x) = \frac{f_\pi}{2\sqrt{2N_c}} (1-2x) \left[1 + 0.55(10x^2 - 10x + 1) \right] , \tag{51}$$

$$\phi_\rho(x) = \frac{3f_\rho}{\sqrt{2N_c}} x(1-x) \left[1 + 0.18C_2^{3/2}(2x-1) \right] , \tag{52}$$

$$\phi_\rho^t(x) = \frac{f_\rho^T}{2\sqrt{2N_c}} \left\{ 3(2x-1)^2 + 0.3(2x-1)^2 [5(2x-1)^2 - 3] \right\}$$

$$+0.21[3 - 30(2x - 1)^2 + 35(2x - 1)^4] \} , \quad (53)$$

$$\phi_\rho^s(x) = \frac{3f_\rho^T}{2\sqrt{2N_c}}(1 - 2x) [1 + 0.76(10x^2 - 10x + 1)] , \quad (54)$$

$$\phi_\rho^T(x) = \frac{3f_\rho^T}{\sqrt{2N_c}}x(1 - x) [1 + 0.2C_2^{3/2}(2x - 1)] , \quad (55)$$

$$\begin{aligned} \phi_\rho^v(x) = & \frac{f_\rho}{2\sqrt{2N_c}} \left\{ \frac{3}{4}[1 + (2x - 1)^2] + 0.24[3(2x - 1)^2 - 1] \right. \\ & \left. + 0.12[3 - 30(2x - 1)^2 + 35(2x - 1)^4] \right\} , \end{aligned} \quad (56)$$

$$\phi_\rho^a(x) = \frac{3f_\rho}{4\sqrt{2N_c}}(1 - 2x) [1 + 0.93(10x^2 - 10x + 1)] , \quad (57)$$

with the Gegenbauer polynomials,

$$\begin{aligned} C_2^{1/2}(t) &= \frac{1}{2}(3t^2 - 1) , & C_4^{1/2}(t) &= \frac{1}{8}(35t^4 - 30t^2 + 3) , \\ C_2^{3/2}(t) &= \frac{3}{2}(5t^2 - 1) , & C_4^{3/2}(t) &= \frac{15}{8}(21t^4 - 14t^2 + 1) . \end{aligned} \quad (58)$$

We shall assume that the ω meson wave functions are identical to the ρ meson ones in this work.

B Factorization Formulas for $B \rightarrow D^* \rho$

In this Appendix we present the factorization formulas for the $B \rightarrow D^* \rho$ decay amplitudes. We parametrize the B , D^* , and ρ meson momenta, and the D^* and ρ meson polarization vectors in the light-cone coordinate as [33]

$$P_1 = \frac{m_B}{\sqrt{2}}(1, 1, \mathbf{0}_T) , \quad P_2 = \frac{m_B}{\sqrt{2}}(1 - r_\rho^2, r^2, \mathbf{0}_T) , \quad P_3 = \frac{m_B}{\sqrt{2}}(r_\rho^2, 1 - r^2, \mathbf{0}_T) , \quad (59)$$

$$\epsilon_2^L = \frac{1}{\sqrt{2}r}(1 - r_\rho^2, -r^2, \mathbf{0}_T) , \quad \epsilon_3^L = \frac{1}{\sqrt{2}r_\rho}(-r_\rho^2, 1 - r^2, \mathbf{0}_T) , \quad (60)$$

$$\epsilon_2^T = \frac{1}{\sqrt{2}}(0, 0, \mp 1, -i) , \quad \epsilon_3^T = \frac{1}{\sqrt{2}}(0, 0, \pm 1, i) , \quad (61)$$

respectively, with $r = m_{D^*}/m_B$ and $r_\rho = m_\rho/m_B$. The fractional momenta of the light valence quarks in the B , D^* and ρ mesons, k_1 , k_2 and k_3 , respectively, are the same as in Eq. (30).

The $B \rightarrow D^* \rho$ decay rates are written as

$$\Gamma_i = \frac{1}{128\pi} G_F^2 |V_{cb}|^2 |V_{ud}|^2 \frac{m_B^3}{r} \sum_{\sigma=L,T} A_i^{(\sigma)\dagger} A_i^{(\sigma)} , \quad (62)$$

where the superscript σ denotes the helicity states of the two vector mesons with $L(T)$ standing for the longitudinal (transverse) component. Similarly, the indices for the classes $i = 1, 2$, and 3 ,

denote the modes $\bar{B}^0 \rightarrow D^{*+}\rho^-$, $\bar{B}^0 \rightarrow D^{*0}\rho^0$, and $B^- \rightarrow D^{*0}\rho^-$, respectively. The amplitude $A_i^{(\sigma)}$ is decomposed into

$$A_i^{(\sigma)} \equiv A_i^L + A_i^N \epsilon_2^*(\sigma = T) \cdot \epsilon_3^*(\sigma = T) + iA_i^T \epsilon^{\alpha\beta\gamma\rho} \epsilon_{2\alpha}^*(\sigma) \epsilon_{3\beta}^*(\sigma) P_{2\gamma} P_{3\rho}, \quad (63)$$

with the convention $\epsilon^{0123} = 1$. The amplitudes A_i^H with the different helicity states $H = L, N, T$ are written as

$$A_1^H = f_\rho \xi_{\text{ext}}^H + f_B \xi_{\text{exc}}^H + \mathcal{M}_{\text{ext}}^H + \mathcal{M}_{\text{exc}}^H, \quad (64)$$

$$A_2^H = -\frac{1}{\sqrt{2}}(f_{D^*} \xi_{\text{int}}^H - f_B \xi_{\text{exc}}^H + \mathcal{M}_{\text{int}}^H - \mathcal{M}_{\text{exc}}^H), \quad (65)$$

$$A_3^H = f_\rho \xi_{\text{ext}}^H + f_{D^*} \xi_{\text{int}}^H + \mathcal{M}_{\text{ext}}^H + \mathcal{M}_{\text{int}}^H. \quad (66)$$

The expressions of the factorizable amplitudes ξ_{ext}^L , ξ_{int}^L , and ξ_{exc}^L are the same as ξ_{ext} , ξ_{int} , and ξ_{exc} in Eqs. (31)-(33), respectively, with the appropriate substitution of the meson masses and of the meson distribution amplitudes. The others are given by

$$\xi_{\text{ext}}^N = \xi_{\text{ext}}^T = 0, \quad (67)$$

$$\begin{aligned} \xi_{\text{int}}^N &= 16\pi C_F \sqrt{r} m_B^2 \int_0^1 dx_1 dx_3 \int_0^{1/\Lambda} b_1 db_1 b_3 db_3 \phi_B(x_1, b_1) \\ &\quad \times r \phi_\rho^T(x_3) E_i(t_i^{(1)}) h(x_1, x_3(1-r^2), b_1, b_3), \end{aligned} \quad (68)$$

$$\begin{aligned} \xi_{\text{int}}^T &= 16\pi C_F \sqrt{r} m_B^2 \int_0^1 dx_1 dx_3 \int_0^{1/\Lambda} b_1 db_1 b_3 db_3 \phi_B(x_1, b_1) \\ &\quad \times 2 r \phi_\rho^T(x_3) E_i(t_i^{(1)}) h(x_1, x_3(1-r^2), b_1, b_3), \end{aligned} \quad (69)$$

$$\xi_{\text{exc}}^N = \xi_{\text{exc}}^T = 0. \quad (70)$$

For the nonfactorizable amplitudes, the expressions of $\mathcal{M}_{\text{ext}}^L$, $\mathcal{M}_{\text{int}}^L$, $\mathcal{M}_{\text{exc}}^L$ are the same as \mathcal{M}_{ext} , \mathcal{M}_{int} , \mathcal{M}_{exc} in Eqs. (39)-(41), respectively, with the appropriate substitution of the meson masses and of the meson distribution amplitudes. The others are given by

$$\mathcal{M}_{\text{ext}}^N = \mathcal{M}_{\text{ext}}^T = 0. \quad (71)$$

$$\mathcal{M}_{\text{int}}^N = \mathcal{M}_{\text{int}}^T = 0. \quad (72)$$

$$\begin{aligned} \mathcal{M}_{\text{exc}}^N &= -32\pi \sqrt{2N} C_F \sqrt{r} m_B^2 \int_0^1 [dx] \int_0^{1/\Lambda} b_1 db_1 b_2 db_2 \phi_B(x_1, b_1) \phi_{D^*}(x_2, b_2) \\ &\quad \times x_2 \phi_\rho^T(x_3) E_f(t_f^{(2)}) h_f^{(2)}(x_i, b_i), \end{aligned} \quad (73)$$

$$\mathcal{M}_{\text{exc}}^T = 0. \quad (74)$$

The factorization formula for the $B \rightarrow D^{*0}\omega$ decay is the same as of the $B \rightarrow D^{*0}\rho^0$ decay with the appropriate substitution of the mass and distribution amplitudes.

References

- [1] M. Bauer, B. Stech, M. Wirbel, Z. Phys. C **29**, 637 (1985); *ibid.* **34**, 103 (1987).
- [2] H.Y. Cheng, Phys. Lett. B **335**, 428 (1994).
- [3] H.Y. Cheng, Z. Phys. C **69**, 647 (1996).
- [4] J. Soares, Phys. Rev D **51**, 3518 (1995); A.N. Kamal and A.B. Santra, Z. Phys. C **72**, 91 (1996); A.N. Kamal, A.B. Santra, and R.C. Verma, Phys. Rev. D **53**, 2506 (1996).
- [5] M. Beneke, G. Buchalla, M. Neubert, and C.T. Sachrajda, Phys. Rev. Lett. **83**, 1914 (1999); Nucl. Phys. **B591**, 313 (2000).
- [6] G.P. Lapage and S.J. Brodsky, Phys. Lett. B **87**, 359 (1979); Phys. Rev. D **22**, 2157 (1980).
- [7] J. Botts and G. Sterman, Nucl. Phys. **B225**, 62 (1989).
- [8] H-n. Li and G. Sterman, Nucl. Phys. **B381**, 129 (1992).
- [9] H-n. Li and H.L. Yu, Phys. Rev. Lett. **74**, 4388 (1995); Phys. Lett. B **353**, 301 (1995); Phys. Rev. D **53**, 2480 (1996).
- [10] C.H. Chang and H-n. Li, Phys. Rev. D **55**, 5577 (1997).
- [11] T.W. Yeh and H-n. Li, Phys. Rev. D **56**, 1615 (1997).
- [12] H.Y. Cheng, H-n. Li, and K.C. Yang, Phys. Rev. D **60**, 094005 (1999).
- [13] H-n. Li, Phys. Rev. D **64**, 014019 (2001); M. Nagashima and H-n. Li, hep-ph/0202127; Phys. Rev. D **67**, 034001 (2003).
- [14] Y.Y. Keum, H-n. Li, and A.I. Sanda, Phys. Lett. B **504**, 6 (2001); Phys. Rev. D **63**, 054008 (2001); Y.Y. Keum and H-n. Li, Phys. Rev. **D63**, 074006 (2001).
- [15] C. D. Lü, K. Ukai, and M. Z. Yang, Phys. Rev. D **63**, 074009 (2001).
- [16] Y.Y. Keum and A. I. Sanda, Phys. Rev. D **67**, 054009 (2003).
- [17] Y.Y. Keum, hep-ph/0210127.
- [18] Y.Y. Keum, hep-ph/0209208.
- [19] M. Neubert and A.A. Petrov, Phys. Lett. B **519**, 50 (2001).
- [20] T. Kurimoto, H-n. Li, and A.I. Sanda, Phys. Rev. D **67**, 054028 (2003).
- [21] A.P. Szczepaniak, E.M. Henley, and S.J. Brodsky, Phys. Lett. B **243**, 287 (1990); G. Burdman and J.F. Donoghue, Phys. Lett. B **270**, 55 (1991).
- [22] J.C. Collins and D.E. Soper, Nucl. Phys. **B193**, 381 (1981).
- [23] H-n. Li, Phys. Rev. D **66**, 094010 (2002).

- [24] T. Kurimoto, H-n. Li, and A.I. Sanda, Phys. Rev. D **65**, 014007, (2002).
- [25] H-n. Li and K. Ukai, Phys. Lett. B **555**, 197 (2003).
- [26] M. Neubert, V. Rieckert, B. Stech and Q.P. Xu, in *Heavy Flavours*, ed. A.J. Buras and M. Lindner (World Scientific, Singapore, 1992) p. 286; M. Neubert and B. Stech, in *Heavy Flavours II*, ed. A.J. Buras and M. Lindner (World Scientific, Singapore, 1998) p. 294, hep-ph/9705292.
- [27] A. Deandrea, N. Di Bartolomeo, R. Gatto, and G. Nardulli, Phys. Lett. B **318**, 549 (1993).
- [28] H.Y. Cheng and K.C. Yang, Phys. Rev. D **59**, 092004 (1999).
- [29] Belle Colla., K. Abe *et al.*, Phys. Rev Lett. **88**, 052002 (2002).
- [30] CLEO Colla., T.E. Coan *et al.*, Phys. Rev. Lett. **88**, 062001 (2002). Phys. Rev. D **59**, 092004 (1999).
- [31] H.Y. Cheng, Phys. Rev. D **65**, 094012 (2002).
- [32] For a review, see G. Buchalla, A.J. Buras, M.E. Lautenbacher, Rev. Mod. Phys. **68**, 1125 (1996).
- [33] C.H. Chen, Y.Y. Keum, and H-n. Li, Phys. Rev. D **64**, 112002 (2001); Phys. Rev. D **66**, 054013 (2002).
- [34] C.Y. Wu, T.W. Yeh, and H-n. Li, Phys. Rev. D **53**, 4982 (1996); *ibid.* **55**, 237 (1997).
- [35] P. Ball, JHEP **01**, 010 (1999).
- [36] P. Ball, V.M. Braun, Y. Koike, and K. Tanaka, Nucl. Phys. B **529**, 323 (1998).
- [37] P. Ball and V.M. Braun, Phys. Rev. D **58**, 094016 (1998); P. Ball, J. High Energy Phys. **9809**, 005 (1998).
- [38] BaBar Colla., B. Aubert *et al.*, hep-ex/0207092.
- [39] M. Gourdin, A.N. Kamal, Y.Y. Keum and X.Y. Pham, Phys. Letts. **B 333**, 507 (1994).
- [40] Z.Z. Xing, hep-ph/0107257.
- [41] C.K. Chua, W.S Hou, and K.C. Yang, Phys. Rev. **D65**, 096007 (2002).
- [42] J.P. Lee, hep-ph/0109101.
- [43] H-n. Li, hep-ph/0110365.
- [44] A. Ali, G. Kramer and C.D. Lü, Phys. Rev. D **58**, 094009 (1998); C.D. Lü, Nucl. Phys. Proc. Suppl. **74**, 227 (1999); Y.H. Chen, H.Y. Cheng, B. Tseng, K.C. Yang, Phys. Rev. **D60**, 094014 (1999).
- [45] K. Hagawara *et al.* (Particle Data Group), Phys. Rev. D **66**, 010001 (2002).

- [46] C.D. LU and K. Ukai, hep-ph/0210206; Y. Li and C.D. Lu, hep-ph/0304288.
[47] C.H. Chen, hep-ph/0302059.

Decay mode	Belle [29]	CLEO [30]
$B^0 \rightarrow D^0 \pi^0$	$3.1 \pm 0.4 \pm 0.5$	$2.74^{+0.36}_{-0.32} \pm 0.55$
$\bar{B}^0 \rightarrow D^{*0} \pi^0$	$2.7^{+0.8+0.5}_{-0.7-0.6}$	$2.20^{+0.59}_{-0.52} \pm 0.79$
$\bar{B}^0 \rightarrow D^0 \eta$	$1.4^{+0.5}_{-0.4} \pm 0.3$	
$\bar{B}^0 \rightarrow D^{*0} \eta$	$2.0^{+0.9}_{-0.8} \pm 0.4$	
$\bar{B}^0 \rightarrow D^0 \omega$	$1.8 \pm 0.5^{+0.4}_{-0.3}$	
$\bar{B}^0 \rightarrow D^{*0} \omega$	$3.1^{+1.3}_{-1.1} \pm 0.8$	

Table 1: Data (in units of 10^{-4}) of the $\bar{B}^0 \rightarrow D^{(*)0} M^0$ ($X = \pi, \eta, \omega$) branching ratios.

Amplitudes	$C_D = 0.6$	$C_D = 0.8$	$C_D = 1.0$
$f_\pi \xi_{\text{ext}}$	6.90	7.46	8.01
$f_D \xi_{\text{int}}$	-1.44	-1.44	-1.44
$f_B \xi_{\text{exc}}$	$-0.01 - 0.03i$	$-0.02 - 0.03i$	$-0.02 - 0.03i$
\mathcal{M}_{ext}	$-0.24 + 0.57i$	$-0.25 + 0.60i$	$-0.27 + 0.65i$
\mathcal{M}_{int}	$3.34 - 3.02i$	$3.22 - 3.07i$	$3.10 - 3.12i$
\mathcal{M}_{exc}	$-0.26 - 0.89i$	$-0.31 - 0.95i$	$-0.37 - 1.02i$

Table 2: Predicted $B \rightarrow D\pi$ decay amplitudes in units of 10^{-2} GeV.

Quantities	$C_D = 0.6$	$C_D = 0.8$	$C_D = 1.0$	Data
\mathcal{M}_1	$6.39 - 0.35i$	$6.88 - 0.38i$	$7.35 - 0.40i$	
\mathcal{M}_2	$-1.53 + 1.48i$	$-1.49 + 1.48i$	$-1.45 + 1.45i$	
\mathcal{M}_3	$8.56 - 2.45i$	$8.99 - 2.47i$	$9.40 - 2.46i$	
$B(B^0 \rightarrow D^+\pi^-)$	2.37	2.74	3.13	3.0 ± 0.4
$B(\bar{B}^0 \rightarrow D^0\pi^0)$	0.26	0.25	0.24	0.29 ± 0.05
$B(B^- \rightarrow D^0\pi^-)$	4.96	5.43	5.91	5.3 ± 0.5
$ a_2/a_1 $ (w/o anni.)	0.47(0.51)	0.43(0.46)	0.39(0.42)	
$Arg(a_2/a_1)$ (w/o anni.)	$-42.5^\circ(-61.5^\circ)$	$-41.6^\circ(-63.5^\circ)$	$-41.9^\circ(-65.3^\circ)$	

Table 3: Predicted $B \rightarrow D\pi$ decay amplitudes in units of 10^{-2} GeV, branching ratios in units of 10^{-3} , $|a_2/a_1|$, and relative angle $Arg(a_2/a_1)$ in units of degree.

Quantities	$C_{D^*} = 0.5$	$C_{D^*} = 0.7$	$C_{D^*} = 0.9$	Data
\mathcal{M}_1	$6.32 - 0.42i$	$6.81 - 0.45i$	$7.30 - 0.49i$	
\mathcal{M}_2	$-1.65 + 1.61i$	$-1.62 + 1.59i$	$-1.59 + 1.57i$	
\mathcal{M}_3	$8.65 - 2.69i$	$9.10 - 2.70i$	$9.55 - 2.70i$	
$B(B^0 \rightarrow D^{*+}\pi^-)$	2.16	2.51	2.88	2.76 ± 0.21
$B(\bar{B}^0 \rightarrow D^{*0}\pi^0)$	0.29	0.28	0.27	0.17 ± 0.05
$B(B^- \rightarrow D^{*0}\pi^-)$	4.79	5.26	5.75	4.60 ± 0.40
$ a_2/a_1 $ (w/o anni.)	0.52 (0.55)	0.47 (0.50)	0.43 (0.47)	
$Arg(a_2/a_1)$ (w/o anni.)	$-40.5^\circ(-61.4^\circ)$	$-40.7^\circ(-63.1^\circ)$	$-40.8^\circ(-64.8^\circ)$	

Table 4: Predicted $B \rightarrow D^*\pi$ decay amplitudes in units of 10^{-2} GeV, branching ratios in units of 10^{-3} , $|a_2/a_1|$, and relative angle $Arg(a_2/a_1)$ in units of degree.

Branching ratios	$C_D = 0.6$	$C_D = 0.8$	$C_D = 1.0$	Data
$B(B^0 \rightarrow D^+\rho^-)$	5.31	6.16	7.06	7.8 ± 1.4
$B(\bar{B}^0 \rightarrow D^0\rho^0)$	0.15	0.15	0.15	
$B(B^- \rightarrow D^0\rho^-)$	8.74	9.85	11.0	13.4 ± 1.8
$B(\bar{B}^0 \rightarrow D^0\omega)$	0.14	0.14	0.14	
Branching ratios	$C_{D^*} = 0.5$	$C_{D^*} = 0.7$	$C_{D^*} = 0.9$	Data
$B(\bar{B}^0 \rightarrow D^{*+}\rho^-)$	4.89	5.67	6.51	7.3 ± 1.5
$B(\bar{B}^0 \rightarrow D^{*0}\rho^0)$	0.41	0.41	0.42	< 0.56
$B(B^- \rightarrow D^{*0}\rho^-)$	10.53	11.72	13.02	15.5 ± 3.1
$B(\bar{B}^0 \rightarrow D^{*0}\omega)$	0.69	0.71	0.75	< 0.74

Table 5: Predicted $B \rightarrow D^{(*)}\rho(\omega)$ branching ratios in units of 10^{-3} .